ALL-PASS FILTERS

NETWORKS, ALL-PASS

FILTERS, ALL-PASS

PHASE EQUALIZERS

All-pass filters are often included in the catalog of classical filter types. A listing of types of classical filters reads as follows: low-pass, high-pass, bandpass, band-stop, and all-pass filters. The transfer functions (see ***Transfer functions***) of all of these filters can be expressed as real, rational functions of the Laplace transform variable s (see ***Laplace transforms***). That is, these transfer functions can be expressed as the ratio of two polynomials in s which have real coefficients. All of the types of filters listed have frequency-selective magnitude characteristics except for the all-pass filter. That is, in the sinusoidal steady state, a low-pass filter passes low-frequency sinusoids relatively well and attenuates high-frequency sinusoids. Similarly, a bandpass filter in sinusoidal steady state passes sinusoids having frequencies that are within the filter's passband relatively well and attenuates sinusoids having frequencies lying outside this band. It should be kept in mind that all of the filters on the list modify the phase of applied sinusoids (see Filtering theory). Figure 1 shows idealized representations of the magnitude characteristics of classical filters for comparison.

However, the all-pass filter is the only filter on the list having a magnitude characteristic that is not frequency selective; in the sinusoidal steady state, an all-pass filter passes sinusoids having any frequency. The filter does not change the amplitude of the input sinusoid or it changes the amplitudes of input sinusoids by the same amount no matter the frequency. An all-pass filter modifies only the phase, and this is the property that is found useful in signal processing.

Only the transfer function of the all-pass filter, expressed as a rational function of s must have zeros (loss poles) in the right-half s plane (*RHP*). The poles and zeros of the transfer function are mirror images with respect to the origin. The transfer functions of the other filters are usually minimum phase transfer functions, meaning that the zeros of these transfer functions are located in the left-half s plane (*LHP*) or on the imaginary axis but not in the open RHP. As a result of these properties, the transfer function of an all-pass filter, $T_{\mathrm{AP}}(s)$, can be expressed as a gain factor H times a ratio of polynomials in which the numerator polynomial can be constructed from the denominator polynomial by replacing s by $-s$ thereby creating zeros that are images of the poles. H can be positive or negative.

The primary application of all-pass filters is in phase equalization of filters having frequency-selective magnitude characteristics. A frequency-selective filter usually realizes an optimum approximation to ideal magnitude characteristics. For example, a Butterworth low-pass filter approximates the ideal brick-wall low-pass magnitude characteristic [see Fig. 1(a)] in a maximally flat manner. An ideal filter also has linear phase in the passband in order to avoid phase distortion. But the Butterworth filter does not have linear phase. So an all-pass filter is designed to be connected in cascade with the Butterworth filter in order to linearize its phase characteristic. This application is discussed in greater detail later in this article.

Another application of all-pass filters is creation of delay for a variety of signal-processing tasks. A signal-processing system may have several branches, and, depending on the application, it may be important to make the delay in each branch approximately equal. This can be done with all-pass filters. On the other hand, a signal processing task may require delaying one signal relative to another. Again, an all-pass filter can be used to provide the delay. This application is also discussed in greater detail in this article.

PROPERTIES OF ALL-PASS FILTERS

The transfer function of an all-pass filter, $T_{\mathrm{AP}}(s)$, has the form

$$T_{\mathrm{AP}}(s) = H\frac{D(-s)}{D(s)} \tag{1}$$

where the constant H is the gain factor, which can be positive or negative, and $D(s)$ is a real polynomial of s. Thus, a first-order all-pass filter transfer function, denoted by T_{AP1}, with a pole on the negative real axis at $s = -a$ is given by

$$T_{\mathrm{AP1}} = H\frac{-s+a}{s+a} \tag{2}$$

and a second-order transfer function, denoted as T_{AP2}, with complex poles described by undamped natural frequency (or natural mode frequency) ω_0 and Q ($\frac{1}{2} < Q < \infty$ for complex poles in the open LHP) is given by

$$T_{\mathrm{AP2}} = H\frac{s^2 - s(\omega_0/Q) + \omega_0^2}{s^2 + s(\omega_0/Q) + \omega_0^2} \tag{3}$$

Of course, an all-pass transfer function can be created that has two real-axis poles as would be obtained by cascading two buffered first-order transfer functions, but all-pass transfer functions with complex poles are the most useful for phase equalization of filters.

To show that the magnitude characteristic is constant for all frequencies for all-pass transfer functions of any order, we first obtain from Eq. (1)

$$T_{\mathrm{AP}}(j\omega) = H\frac{D(-j\omega)}{D(j\omega)} = H\frac{D^*(j\omega)}{D(j\omega)} \tag{4}$$

where $*$ indicates the conjugate. Then from Eq. (4), we obtain

$$|T_{\mathrm{AP}}(j\omega)| = |H|\frac{|D^*(j\omega)|}{|D(j\omega)|} = |H| \tag{5}$$

This result is also shown graphically in Fig. 2 for the case of a second-order all-pass transfer function with complex poles. An arbitrary point P has been selected on the $j\omega$ axis, and we see that the lengths of the vectors from the poles to

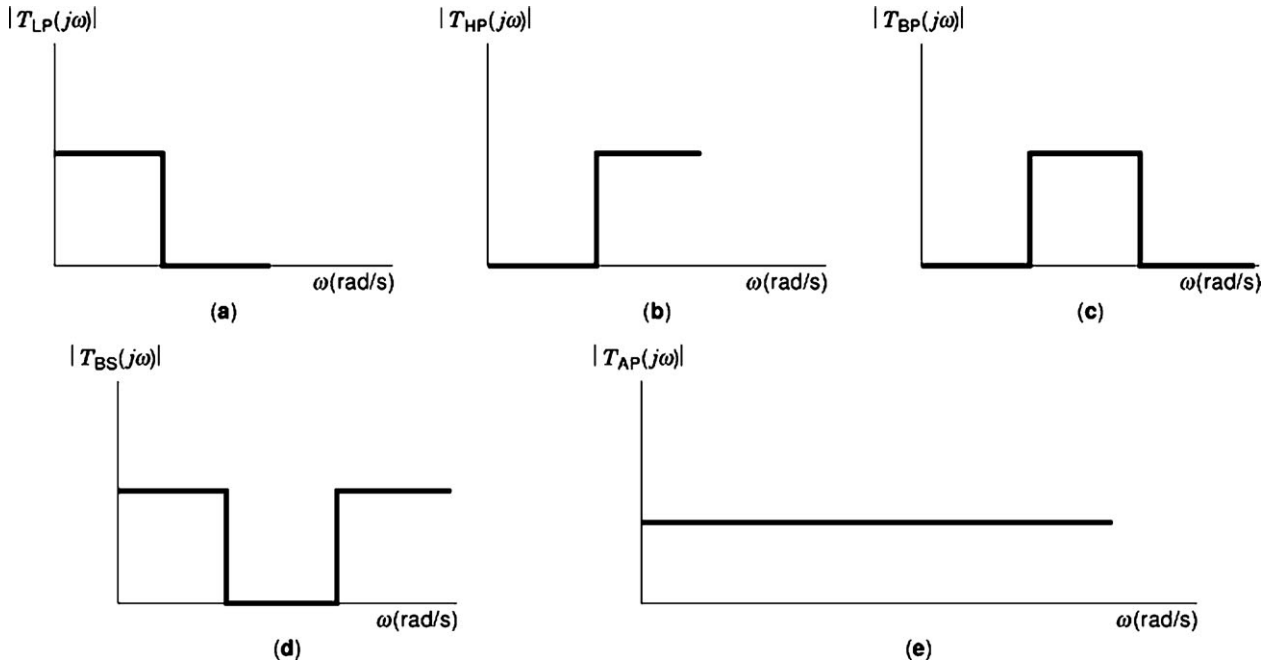

Figure 1. Idealized magnitude characteristics of classical filters. (a) Low-pass filter. (b) High-pass filter. (c) Bandpass filter. (d) Band-stop filter. (e) All-pass filter.

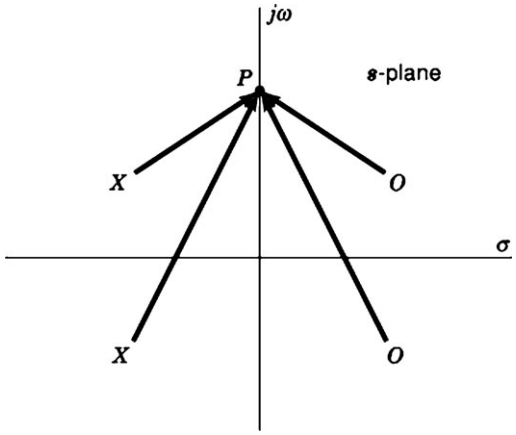

Figure 2. A pole-zero plot for a second-order all-pass transfer function with complex poles is shown. An arbitrary point on the $j\omega$ axis, denoted as P, has been selected. The lengths of the vectors from the poles to point P are the same as the corresponding lengths of the vectors from the zeros to point P

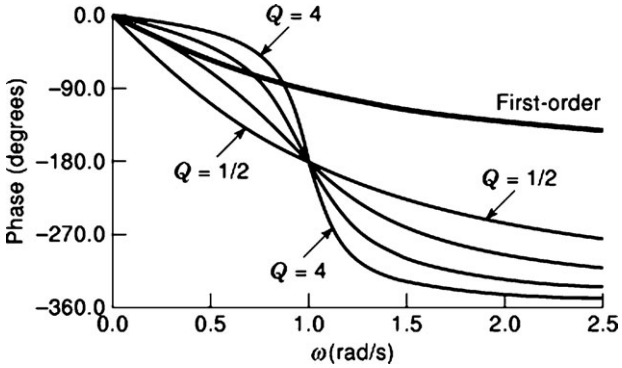

Figure 3. Phase plots for the first-order all-pass transfer function of Eq. (2) with a zero at $s = 1$ and for second-order transfer functions of Eq. (3) with $\omega_0 = 1$ and $Q = ½, 1, 2$, and 4. H is positive for all the transfer functions.

the point are the same as the lengths of the vectors from the zeros to point P. Thus, the magnitude characteristic is determined only by H and is not a function of frequency.

The phase, however, is a function of frequency. Denoting the phase of the all-pass transfer function as θ_{AP}, selecting H to be positive for convenience, and denoting the phase of $D(j\omega)$ as θ_D, we can write:

$$\theta_{AP}(\omega) = -2\theta_D(\omega) \tag{6}$$

The all-pass transfer function produces phase lag, see 1. If H is negative, then an additional phase of π radians is introduced. Figure 3 shows the phase plots obtained for the first-order transfer function in Eq. (2) with $a = 1$ and for the second-order transfer function in Eq. (3) with $\omega_0 = 1$ and Q values equal to ½, 1, 2, and 4. H is positive for all the transfer functions. Upon examination of the plots generated by the second-order transfer functions, it is seen that for $Q = ½$, there is no point of inflection. For certain higher values of Q, there is a point of inflection. The point of inflection is obtained by differentiating the expression for phase two times with respect to ω, equating the result to zero, and solving for a positive ω. The result is

$$\omega = \sqrt{\sqrt{4 - \frac{1}{Q^2}} - 1}, \quad Q \geq \frac{1}{\sqrt{3}} \tag{7}$$

Thus, for Qs greater than 0.578, there is a point of inflection in the phase plot.

The negative of the derivative of phase with respect to ω is the group delay, denoted as $\tau(\omega)$. Group delay is also

termed envelope delay or merely delay, and its units are seconds. Oftentimes, designers prefer working with delay rather than phase because delay can be expressed as a rational function of ω. The expression for phase involves a transcendental function $\tan^{-1}(\ )$. For example, the phase of the second-order transfer function with positive H, $\omega_0 = 1$ and $Q = 2$ (see Eq. 3) is

$$\theta_{AP}(\omega) = -2\tan^{-1}\frac{\frac{\omega\omega_0}{Q}}{\omega_0^2 - \omega^2} = -2\tan^{-1}\frac{0.5\omega}{1-\omega^2} \tag{8}$$

However, the delay is given by

$$\tau(\omega) = -\frac{d\theta_{AP}(\omega)}{d\omega} = \frac{1+\omega^2}{1-(7/4)\omega^2+\omega^4} \tag{9}$$

which is a rational function of ω resulting from the derivative of the arctangent function. Figure 4 depicts the delays corresponding to the phase plots given in Fig. 3. For Q greater than 0.578, the plots of delay exhibit peaks. For $Q^2 > \frac{1}{2}$, the peaks occur at $\omega \cong \omega_0 = 1$.

PHASE DISTORTION

At steady state, a linear, time-invariant network affects only the amplitude and phase of an applied sinusoid to produce an output sinusoid. The output sinusoid has the same frequency as the input sinusoid. If the input signal is composed of two sine waves of different frequencies, then, depending on the network, the output signal could be changed in amplitude or in phase or both. For example, suppose the network is a low-pass filter and that the input signal consists of two sinusoids with different frequencies, but both frequencies lie within the passband. In this case, the network should pass the signal to the output with minimum distortion. Since the frequencies of the sine waves that make up the input signal lie within the passband, very little amplitude distortion is encountered. However, the result can be severely phase distorted. If no phase distortion is to be produced, then the phase characteristic in the passband of the network must be linear and, hence, have the form $-k\omega + \theta_0$, where k is the magnitude of the slope of the phase characteristic and θ_0 is the phase at $\omega = 0$. Furthermore, if θ_0 is neither 0 nor a multiple of 2π radians, then a distortion known as phase-intercept distortion results. In the following, phase-intercept distortion is not considered. The interested reader is referred to Ref. 2 for further information on phase-intercept distortion.

To illustrate the effects that a system with linear phase has on an input signal, let an input signal $v(t)$, given by

$$v(t) = A_1\sin(\omega t) + A_2\sin(2\omega t) \tag{10}$$

be applied to a network with transfer function $T(s)$. Assume the phase of the system is given by $\theta(\omega) = -k\omega$, where k is a positive constant, and assume that $|T(j\omega)| = |T(2j\omega)| = 1$. In Eq. (10), A_1 and A_2 are the peak amplitudes of the two sinusoids that make up $v(t)$. The output signal can be written as

$$v_o(t) = A_1|T(j\omega)|\sin(\omega t - k\omega) + A_2|T(2j\omega)|\sin(2\omega t - 2k\omega) \tag{11}$$

Rewriting Eq. (11), we obtain

$$v_o(t) = A_1\sin\omega(t-k) + A_2\sin 2\omega(t-k) \tag{12}$$

where it is seen that each sinusoid in $v_o(t)$ is delayed by the same amount, namely k seconds. The output voltage has been delayed by k seconds, but there is no phase distortion.

However, suppose the phase of the system is given by $\theta = -k\omega^3$, a nonlinear phase characteristic. With the input signal given by Eq. (10) and, as before, assuming that $|T(j\omega)| = |T(2j\omega)| = 1$, we obtain

$$v_o(t) = A_1\sin\omega(t-k\omega^2) + A_2\sin 2\omega(t-4k\omega^2) \tag{13}$$

From Eq. (13), it is seen that the sinusoids are delayed by different amounts of time. The nonlinear phase characteristic has resulted in phase distortion. Although the human ear is relatively insensitive to phase changes (3), applications such as control and instrumentation can be greatly impaired by phase distortion. To illustrate this important point further, assume that a signal $v_i(t)$ is applied to three different hypothetical amplifiers. The signal $v_i(t)$ is composed of two sinusoids and is given by

$$v_i(t) = 0.1\sin(t) + 0.05\sin(2t) \tag{14}$$

One sinusoid has twice the frequency of the other sinusoid. One amplifier is perfectly ideal and has a gain $G_1 = 10$ with no phase shift. The second amplifier has a gain magnitude equal to 10 and has a linear phase shift given by $\theta = -\omega$. Thus, its transfer function can be expressed as

$$G_2(j\omega) = 10e^{-j\omega} \tag{15}$$

The third amplifier also has a gain magnitude equal to 10, but it has a nonlinear phase characteristic given by $\theta = -\omega^3$. Thus, its transfer function is given by

$$G_3(j\omega) = 10e^{-j\omega^3} \tag{16}$$

Figure 5 depicts the output of the first amplifier. Since the amplifier is perfectly ideal, the output is exactly $10v_i$. Figure 6 shows the output of the second amplifier, and it is seen that the waveform at the output of the amplifier with linear phase is the same as shown in Fig. 5 except that the waveform in Fig. 6 has been delayed by 1 s. Delay of the entire waveform does not constitute phase distortion. On the other hand, the output of the amplifier with nonlinear phase, shown in Fig. 7, is clearly distorted. For example, its peak-to-peak value is more than 12% larger than it should be. In the next section, we examine the use of a second-order all-pass filter to linearize the phase of nth-order low-pass filters.

PHASE EQUALIZATON

Phase equalization is the term used to describe compensation employed with a filter or a system to remedy phase distortion. The goal is to achieve linear phase (flat time delay), and the compensator is labeled a phase equalizer. In this section, we derive the specifications for a second-order all-pass filter that can be used to linearize the phase of most all-pole low-pass filters. The technique can also be

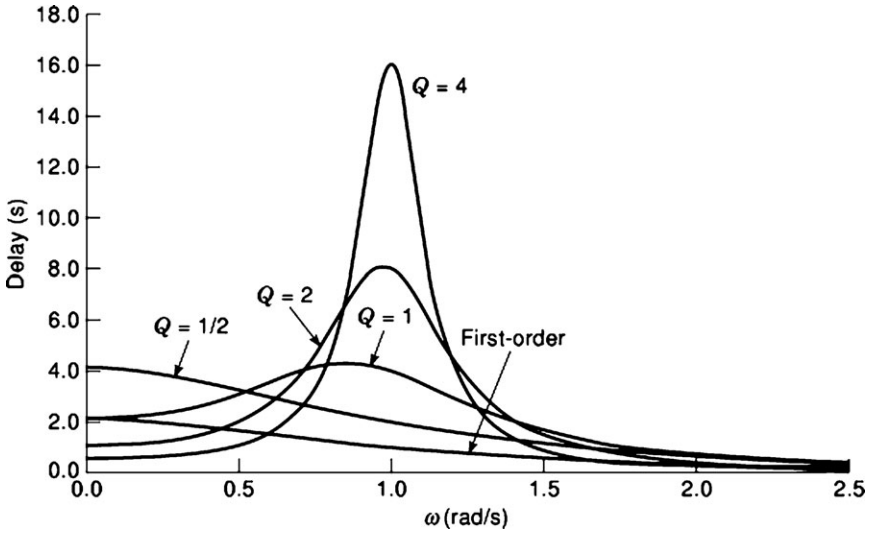

Figure 4. Delay plots for the all-pass transfer functions listed in Fig. 3. The plot for $Q = \frac{1}{2}$ has the largest delay near the origin.

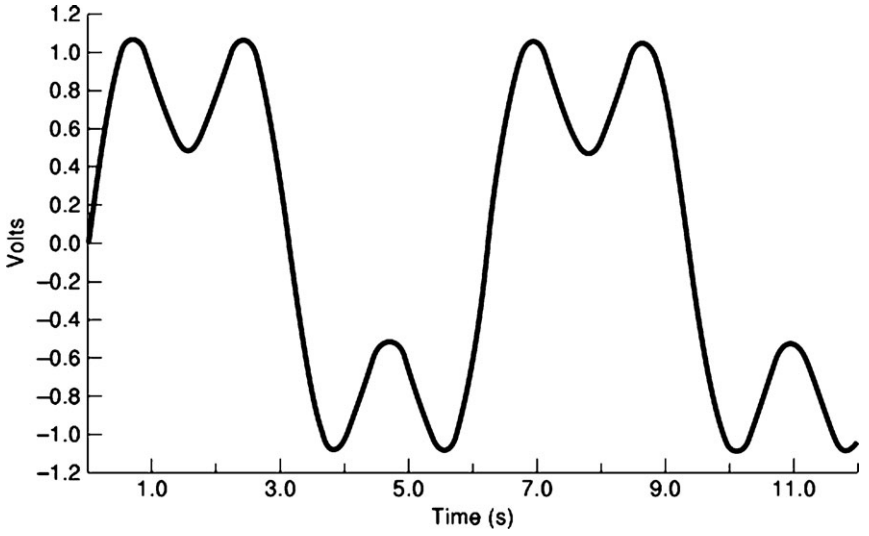

Figure 5. Output voltage of perfectly ideal amplifier with input voltage given by Eq. (14). The amplifier has a gain equal to 10 with no phase shift.

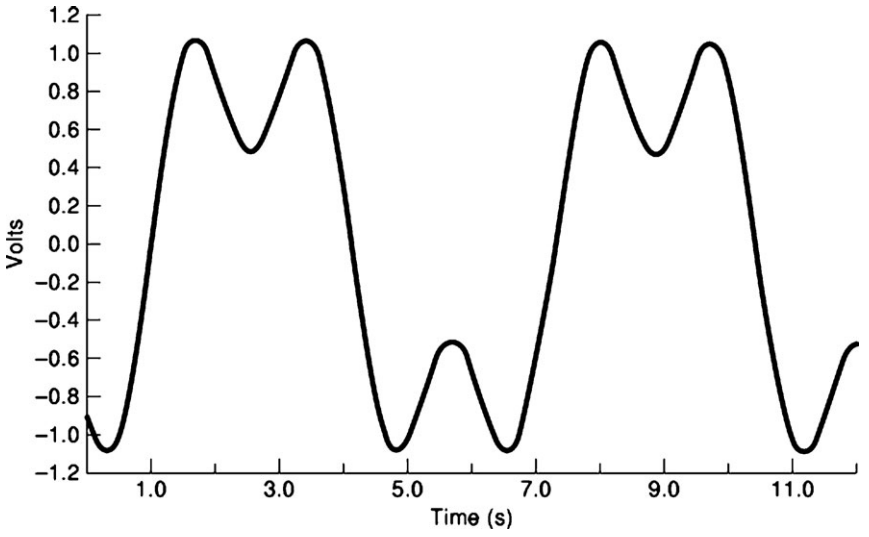

Figure 6. Output voltage of amplifier with linear phase characteristic. The output voltage is delayed 1 s in comparison to the output voltage shown in Fig. 5.

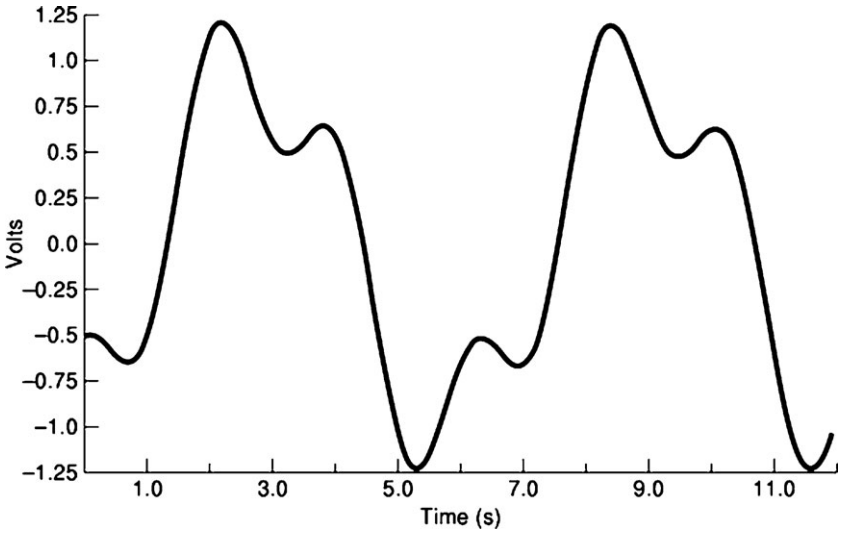

Figure 7. Output voltage of amplifier with nonlinear phase characteristic with input voltage given by Eq. (14). The effects of phase distortion are easily seen when this waveform is compared with those in Figs. 5 and 6.

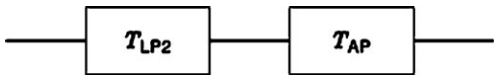

Figure 8. Cascade connection of a second-order low-pass filter with a second-order all-pass filter. It is assumed there is no loading between the two filters.

extended to other phase-equalization tasks. We begin the derivation by linearizing the phase of a second-order low-pass filter having a transfer function given by

$$T_{LP2}(s) = \frac{\omega_1^2}{s^2 + s(\omega_1/Q_1) + \omega_1^2} \tag{17}$$

Figure 8 depicts the cascade connection of this low-pass filter with a second-order all-pass filter with transfer function $T_{AP}(s)$. The form of the transfer function of the all-pass filter is given by Eq. (3), but for the purposes of this derivation, let us designate its undamped natural frequency as ω_A and its Q as Q_A. The overall phase of the cascade circuit is $\theta(\omega) = \theta_L(\omega) + \theta_A(\omega)$ where θ_L and θ_A are the phase contributed by the low-pass filter and the all-pass filter, respectively. We wish to make $\theta(\omega)$ approximate linear phase in the Maclaurin sense (1). Since θ is an odd function of ω, the Maclaurin series for θ has the form

$$\theta(\omega) = K_1\omega + K_3\omega^3 + K_5\omega^5 + K_7\omega^7 + \cdots \tag{18}$$

where K_1 is the first derivative of $\theta(\omega)$ with respect to ω with the result evaluated at $\omega = 0$, and K_3 is proportional to the third derivative evaluated at $\omega = 0$, and so on. Therefore, we want to choose ω_A and Q_A to make K_3 and K_5 equal to zero in Eq. (18). Then $K_7\omega^7$ will be the lowest order undesired term in the series for $\theta(\omega)$.

The phase θ_L contributed by the second-order low-pass filter can be expressed as

$$\theta_L = -\tan^{-1}\left[\frac{\dfrac{1}{Q_1}\dfrac{\omega}{\omega_1}}{1-\left(\dfrac{\omega}{\omega_1}\right)^2}\right] \tag{19}$$

The use of a program that is capable of performing symbolic algebra is recommended to obtain the Maclaurin series for θ_L. The results are

$$\theta_L = -\frac{1}{Q_1}\left(\frac{\omega}{\omega_1}\right) - \left(\frac{1}{Q_1} - \frac{1}{3Q_1^3}\right)\left(\frac{\omega}{\omega_1}\right)^3 - \left(\frac{1}{Q_1} - \frac{1}{Q_1^3} + \frac{1}{5Q_1^5}\right)\left(\frac{\omega}{\omega_1}\right)^5 - \left(\frac{1}{Q_1} - \frac{2}{Q_1^3} + \frac{1}{Q_1^5} - \frac{1}{7Q_1^7}\right)\left(\frac{\omega}{\omega_1}\right)^7 + \cdots \tag{20}$$

Equation (20) can be used also to write the series for the phase of the all-pass filter directly. Then, forming $\theta = \theta_L + \theta_A$ and truncating the results after the term containing ω^7 we obtain

$$\begin{aligned}\theta(\omega) \approx\ & -\left(\frac{1}{Q_1\omega_1} + \frac{2}{Q_A\omega_A}\right)\omega - \left[\left(\frac{1}{Q_1} - \frac{1}{3Q_1^3}\right)\frac{1}{\omega_1^3} + \left(\frac{1}{Q_A} - \frac{1}{3Q_A^3}\right)\frac{2}{\omega_A^3}\right]\omega^3 \\ & - \left[\left(\frac{1}{Q_1} - \frac{1}{Q_1^3} + \frac{1}{5Q_1^5}\right)\frac{1}{\omega_1^5} + \left(\frac{1}{Q_A} - \frac{1}{Q_A^3} + \frac{1}{5Q_A^5}\right)\frac{2}{\omega_A^5}\right]\omega^5 \\ & - \left[\left(\frac{1}{Q_1} - \frac{2}{Q_1^3} + \frac{1}{Q_1^5}\right)\frac{1}{\omega_1^7} + \left(\frac{1}{Q_A} - \frac{2}{Q_A^3} + \frac{1}{Q_A^5}\right)\frac{2}{\omega_A^7}\right]\omega^7\end{aligned} \tag{21}$$

The next step is to set the coefficients of ω^3 and ω^5 equal to zero in Eq. (21). Thus, we must satisfy the equations

$$-\frac{1}{2\omega_1^3}\left(\frac{1}{Q_1} - \frac{1}{3Q_1^3}\right) = \left(\frac{1}{Q_A} - \frac{1}{3Q_A^3}\right)\frac{1}{\omega_A^3} \tag{22a}$$

$$-\frac{1}{2\omega_1^5}\left(\frac{1}{Q_1} - \frac{1}{Q_1^3} + \frac{1}{5Q_1^5}\right) = \left(\frac{1}{Q_A} - \frac{1}{Q_A^3} + \frac{1}{5Q_A^5}\right)\frac{1}{\omega_A^5} \tag{22b}$$

Introduce parameters a and b to represent the left sides of Eqs. 22a and 22b, respectively. That is, let

$$a = -\frac{1}{2\omega_1^3}\left(\frac{1}{Q_1} - \frac{1}{3Q_1^3}\right) \tag{23a}$$

$$b = -\frac{1}{2\omega_1^5}\left(\frac{1}{Q_1} - \frac{1}{Q_1^3} + \frac{1}{5Q_1^5}\right) \tag{23b}$$

Thus, we have two equations, Eqs. 22a and 22b, that involve a, b, Q_A, and ω_A. Upon eliminating ω_A, we obtain a twelfth-order equation for Q_A given by

$$Q_A^{12} - (3+d)Q_A^{10} + \left(\frac{18}{5} + \frac{5}{3}d\right)Q_A^8 - \left(\frac{11}{5} + \frac{10}{9}d\right)Q_A^6 + \left(\frac{18}{25} + \frac{10}{27}d\right)Q_A^4 - \left(\frac{3}{25} + \frac{5}{81}d\right)Q_A^2 + \left(\frac{1}{125} + \frac{1}{243}d\right) = 0 \tag{24}$$

where

$$d = \frac{b^3}{a^5} \tag{25}$$

For a given second-order low-pass transfer function, d can be found from Eqs. 23a, and 23b. Then a positive solution for Q_A is sought from Equation (24). Finally, ω_A is obtained from

$$\omega_A = \left[\frac{1}{a}\left(\frac{1}{Q_A} - \frac{1}{3Q_A^3}\right)\right]^{1/3} \tag{26}$$

Note that a positive result must be found both for Q_A from Eq. (24) and for ω_A from Eq. (26) in order to obtain a solution.

Although only a second-order low-pass filter transfer function was utilized to derive Eqs. 24 and 26, these two equations are used for the nth order all-pole case as well because only the parameters a, b, and d need to be modified. For example, suppose we wish to linearize the phase of a normalized fourth-order Butterworth filter, denoted as $B_4(s)$, with a second-order all-pass filter. The transfer function $B_4(s)$ is given by

$$B_4(s) = \frac{\omega_1^2\omega_2^2}{\left(s^2 + s\frac{\omega_1}{Q_1} + \omega_1^2\right)\left(s^2 + s\frac{\omega_2}{Q_2} + \omega_2^2\right)} \tag{27}$$

where $\omega_1 = \omega_2 = 1$, $Q_1 = 0.541196$, and $Q_2 = 1.306563$. The parameters a and b become

$$a = -\frac{1}{2\omega_1^3}\left(\frac{1}{Q_1} - \frac{1}{3Q_1^3}\right) - \frac{1}{2\omega_2^3}\left(\frac{1}{Q_2} - \frac{1}{3Q_2^3}\right) = -0.1803987 \tag{28a}$$

$$b = -\frac{1}{2\omega_1^5}\left(\frac{1}{Q_1} - \frac{1}{Q_1^3} + \frac{1}{5Q_1^5}\right) - \frac{1}{2\omega_2^5}\left(\frac{1}{Q_2} - \frac{1}{Q_2^3} + \frac{1}{5Q_2^5}\right) = -0.1082392 \tag{28b}$$

Calculating d from Eq. (25) and employing Eqs. 24 and 26, we obtain $Q_A = 0.5434$ and $\omega_A = 1.0955$. If the normalized Butterworth transfer function is to be frequency scaled to a practical frequency, then the all-pass transfer function must be frequency scaled by the same amount.

Phase equalization has been applied only to transfer functions of even order in the derivation and the example. To apply phase equalization to an odd-order filter, we must determine the additional factor to add to each parameter a and b. An odd-order, all-pole, low-pass filter transfer function $T_o(s)$ can be expressed as $T_o(s) = T_1(s)T_E(s)$ where $T_1(s)$ is given by

$$T_1(s) = \frac{k}{s+k} \tag{29}$$

k is positive, and $T_E(s)$ is the remaining portion of the overall transfer function and is of even order. We have assumed that the odd order of $T_o(s)$ arises because of the existence of one real axis pole, the usual case. All other poles of $T_o(s)$ occur in complex conjugate pairs. Denoting the phase of $T_1(j\omega)$ as $\theta_1(\omega)$, we write

$$\theta_1(\omega) = -\tan^{-1}\frac{\omega}{k} \tag{30}$$

If we consider the case of linearizing the phase given in Eq. (30) with a second-order all-pass transfer function, we obtain

$$a = \frac{1}{6k^3}, \quad b = -\frac{1}{10k^5} \tag{31}$$

and the terms given in Eq. (31) are added to the expressions for the parameters a and b for higher order odd transfer functions.

Table 1. All-Pass Filter Constants for Phase Equalization of Butterworth and Chebyshev Filters

Order	Q_A	ω_A
Butterworth (3.01-dB Passband Variation)		
2	– (no solution)	–
3	0.5509	1.0232
4	0.5434	1.0955
5	0.5406	1.0812
6	0.5389	1.0520
7	0.5377	1.0208
8	0.5368	0.9910
9	0.5361	0.9635
Chebyshev (1-dB Passband Ripple)		
2	0.5326	1.0460
3	0.6433	0.6405
4	0.5169	0.6094
5	0.6443	0.3766
6	0.5099	0.4311
7	0.6450	0.2675
8	0.5064	0.3326
9	0.6453	0.2075

Table 1 provides the values for Q_A and ω_A needed to linearize the phase of low-pass Butterworth filters with a 3.01-dB variation in the passband and the phase of 1-dB ripple Chebyshev low-pass filters. Note that no solution exists for the second-order Butterworth filter. As an application of Table 1, we find the step responses of two normalized fifth-order Butterworth filters. One filter has a second-order all-pass connected in cascade in order to linearize its phase, and the other does not. The transfer function $B_5(s)$ is given by

$$B_5(s) = \frac{1}{(s+1)[s^2 + 0.618034s + 1][s^2 + 1.618034s + 1]} \tag{32}$$

In Fig. 9, the step response of $B_5(s)$ has less delay, and the step response of $B_5(s)T_{AP2}(s)$ with Q_A and ω_A obtained from

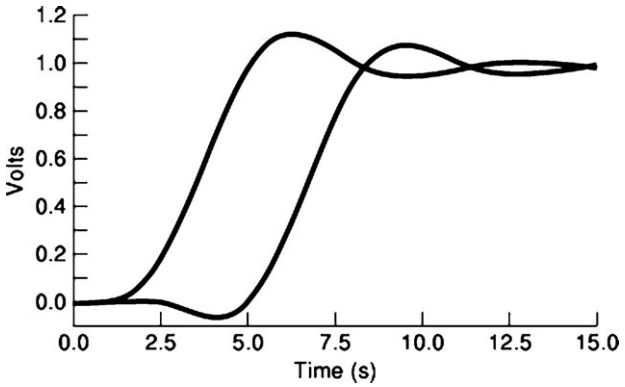

Figure 9. Step responses of fifth-order Butterworth low-pass filters with and without phase equalization. The step response of the filter with phase equalization exhibits preshoot and has greater delay.

Table 1 has greater delay due to the presence of the all-pass filter. However, it is seen from Fig. 9 that the response for the phase-equalized filter more nearly approximates the step response of an ideal low-pass filter with delay because the response of an ideal filter should begin ringing before it rises to the upper amplitude level. In other words, it should exhibit "preshoot."

Oftentimes, the design of filters having frequency-selective magnitude characteristics other than low-pass is accomplished by applying Cauer transformations to a low-pass prototype transfer function. Unfortunately, the Cauer transformations do not preserve the phase characteristics of the low-pass transfer function. Thus, if a Cauer low-pass to bandpass transformation is applied to a low-pass filter transfer function that has approximately linear phase, the resulting bandpass filter transfer function cannot be expected to have linear phase, especially if the bandwidth of the bandpass filter is relatively wide. An approach to linearizing the phase of filters other than low-pass filters is to make use of a computer program that plots delay resulting from the cascading of a specified magnitude-selective filter with one or more all-pass filters. Using Eq. (7) and Figure 4 as guides, the peaks of the time delays of the all-pass filters can be placed to achieve approximately linear overall phase.

AN APPLICATION OF DELAY

An all-pass filter can be combined with a comparator to obtain a slope-polarity detector circuit (4). The basic arrangement of the all-pass filter and the comparator is shown in Fig. 10. An LM311 comparator works well in this circuit, and a first-order all-pass filter can be used for input signals that are composed of sinusoids that do not differ greatly in frequency. To understand the behavior of this circuit, suppose $v_i(t) = A\sin(\omega t)$, where A is positive and represents the peak value of the sine wave. The output voltage of the all-pass filter is $v_A(t) = A\sin(\omega t\text{-}\omega t_1)$, where t_1 is the delay in seconds caused by the filter. Figure 11 depicts $v_i(t)$, $v_A(t)$, and the output voltage of the comparator $v_o(t)$, for $A = 4$ V and $\omega = 2\pi(100)$ rad/s. The output terminal of the comparator has a pull-up resistor connected to 5 V. Ideally, when the

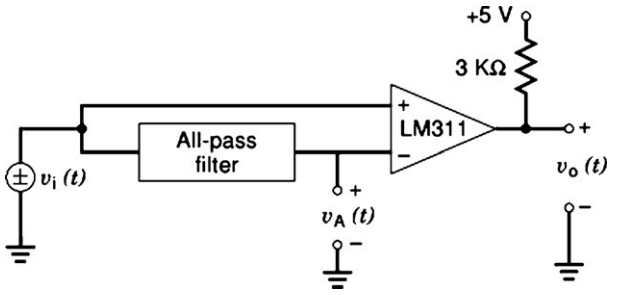

Figure 10. Essential components of a slope-polarity detector.

slope of $v_i(t)$ is positive, $v_o(t)$ is high, and $v_o(t)$ is low when the slope of $v_i(t)$ is negative. Actually, the circuit's output changes state at a time which is slightly past the time at which $v_i(t)$ changes slope. It is at this later time that the delayed input to the comparator, $v_A(t)$, causes the polarity of the voltage $(v_i(t) - v_A(t))$ between the leads of the comparator to change. The need for an all-pass filter in this application is clear because the amplitude of the input signal must not be changed by the delaying circuit no matter the frequencies present in the input signal. A first-order all-pass filter is ordinarily adequate for the task. The pole and zero can be set far from the origin, and their placement is not overly critical. Too little delay results in insufficient overdrive for the comparator. Too much delay increases the error in the time at which the comparator changes state because the polarity of the voltage between the leads of the comparator does not change soon enough after the slope of $v_i(t)$ changes. For the example illustrated in Fig. 11 involving a simple sine wave, the amplitudes of the input and delayed sine waves are equal at a time closest to zero denoted by t_E and given by

$$t_E = \frac{1}{2}\left(\frac{\pi}{\omega} + t_1\right) \tag{33}$$

The voltage difference, denoted as V_E, between the peak of the input sine wave and the level at which the input and delayed sine waves are equal is given by

$$V_E = A\left(1 - \cos\frac{\omega t_1}{2}\right) \approx A\frac{\omega^2 t_1^2}{8} \tag{34}$$

If, for example, the delay provided by the all-pass filter is 0.5 ms for the 100-Hz input sine wave, then the input sine wave will have decreased by approximately 50 mV from its peak value before the comparator begins to change state. This circuit works well at steady state for input signals that do not contain significant high-frequency components. Thus, it works reasonably well if the input signal is a triangular waveform, but it does not work well with square waves.

A SYNTHESIS APPLICATION

First-order all-pass filters can be utilized to realize filters with magnitude-selective characteristics. For example, the circuit shown in Fig. 12, which is based on (5) and (6), realizes a bandpass filter transfer function by using a first-order all-pass circuit in a feedback loop. The overall trans-

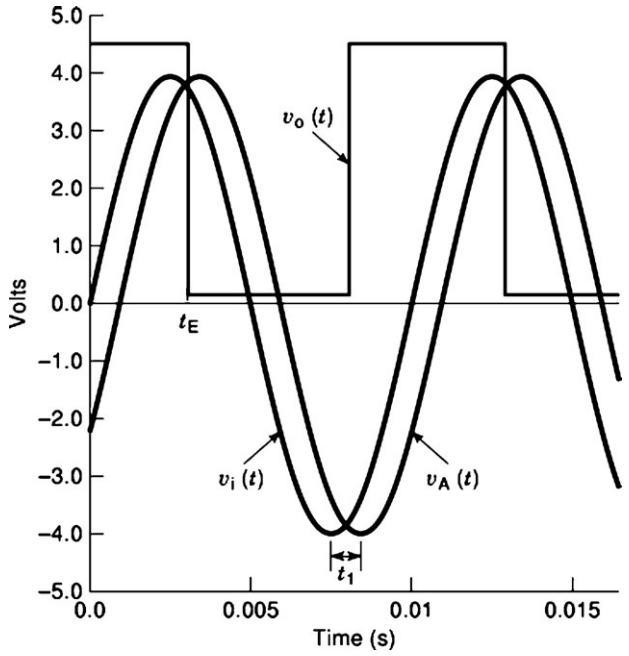

Figure 11. Input voltage $v_i(t)$, delayed input voltage $v_A(t)$, and comparator output voltage $v_o(t)$ for the slope-polarity detector shown in Figure 10 when the input voltage is a sine wave.

fer function of the circuit is

$$\frac{V_0}{V_i} = \frac{-\frac{s}{C_3R_1}\left(s+\frac{1}{CR}\right)}{\left(s+\frac{1}{C_1R_1}\right)\left[s^2+s\left(\frac{1}{C_3R_3}+\frac{1}{CR}-\frac{K_1}{C_3R_2}\right)+\frac{1+K_1\frac{R_3}{R_2}}{CRC_3R_3}\right]} \tag{35}$$

where K_1 is the gain factor associated with the transfer function of the first-order all-pass filter. If $C_1R_1 = CR$, $K_1 = 1$, and $R_2 = R_3$, then Eq. (35) reduces to the transfer function of a standard second-order bandpass filter given by

$$\frac{V_0}{V_i} = \frac{-\frac{s}{C_3R_1}}{s^2+\frac{s}{C_1R_1}+\frac{2}{C_1C_3R_1R_3}} \tag{36}$$

The Q and ω_0 of the poles in Eq. (36) are

$$Q = \sqrt{\frac{2C_1R_1}{C_3R_3}}, \quad \omega_0 = \sqrt{\frac{2}{C_1C_3R_1R_3}} \tag{37}$$

Although the circuit requires the matching of elements and several operational amplifiers, including, possibly, a buffer at the input, it demonstrates that all-pass filters can be employed in the realization of filters having frequency-selective magnitude characteristics.

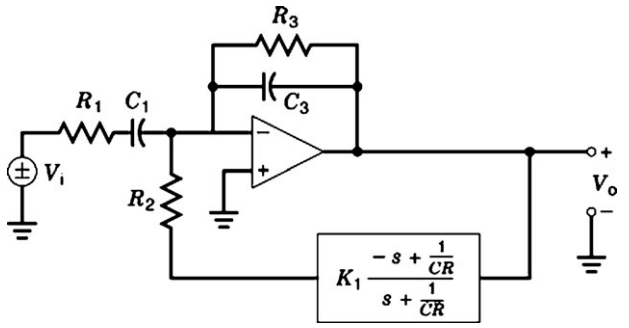

Figure 12. Second-order bandpass filter realized by incorporating a first-order all-pass filter in a feedback path.

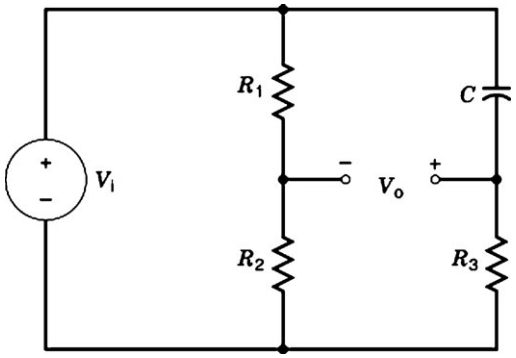

Figure 13. Passive circuit that can be used to realize a first-order all-pass filter. Only one capacitor is needed.

ALL-PASS CIRCUIT REALIZATIONS

Voltage-mode Realizations

In this section, we examine a variety of circuits used to realize all-pass transfer functions for which the input and output variables of interest are voltage. Inductorless circuits for first-order all-pass filters can be realized using the bridge circuit shown in Fig. 13. The transfer function of this circuit is given by

$$\frac{V_0}{V_i} = -\frac{-s\left(\frac{R_1}{R_1+R_2}\right)+\frac{R_2}{CR_3(R_1+R_2)}}{s+\frac{1}{CR_3}} \tag{38}$$

If $R_1 = R_2$, then Eq. (38) reduces to the transfer function of an all-pass filter (7). However, the requirement that $R_1 = R_2$ results in a gain factor equal to $-½$, which is small in magnitude. Also, a common ground does not exist between the input and output ports of the circuit.

The bridge circuit shown in Fig. 14, which can be redrawn as a symmetrical lattice, can realize first-order all-pass transfer functions with a gain factor equal to 1. The transfer function of this circuit is

$$\frac{V_0}{V_i} = \frac{Z_A - Z_B}{Z_A + Z_B} \tag{39}$$

If $Z_B = R$ and $Z_A = 1/(sC)$, a first-order all-pass transfer function is obtained. If inductors are allowed in the circuit, then the circuit in Fig. 14 can realize higher order all-pass

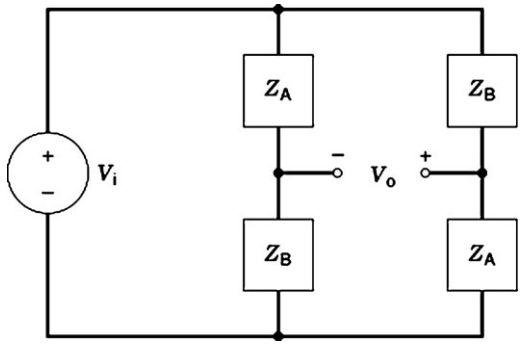

Figure 14. Passive circuit that can be used to realize first-order all-pass filters with gain factor equal to 1. Two capacitors are needed. If inductors are allowed, this circuit can realize higher order all-pass transfer functions with complex poles.

transfer functions. For example, suppose a circuit is needed to realize a third-order all-pass transfer function $T_{AP3}(s)$ given by

$$T_{AP3} = \frac{-s^3 + s^2 - 2s + 1}{s^3 + s^2 + 2s + 1} = \frac{p(s)}{q(s)} \tag{40}$$

where $p(s)$ and $q(s)$ are the numerator and denominator polynomials, respectively. The denominator polynomial $q(s)$ can be expressed as the sum of its even part, $m(s)$, and its odd part, $n(s)$. Thus, $q(s) = m(s) + n(s)$. If the roots of $q(s)$ are confined to the open LHP, then the ratios n/m and m/n meet the necessary and sufficient conditions to be an LC driving point impedance (8). Thus, if the numerator and denominator of the transfer function in Eq. (40) are divided by $m(s)$, we obtain

$$T_{AP3} = \frac{1 - [(s^3 + 2s)/(s^2 + 1)]}{1 + [(s^3 + 2s)/(s^2 + 1)]} \tag{41}$$

By comparing the result in Eq. (41) with Eq. (39), it is seen that $Z_A = 1\ \Omega$ and the box labeled Z_B in Fig. 14 consists of the series connection of a 1 Henry inductor and an LC tank circuit that resonates at 1 rad/s. However, the resulting circuit requires six reactive elements and does not have a common ground between the input and output ports, and these properties may preclude the use of bridge circuit all-pass networks in some applications.

Single transistor first-order all-pass transfer function realizations have been described by several authors. The interested reader may refer to Refs. 9 and 10 for additional information. Inductorless second-order realizations are also described in Refs. 9 and 10 but the poles and zeros of the transfer functions are confined to the real axis. Rubin and Even extended the results in Ref. 9 to include higher order all-pass transfer functions with complex poles, but inductors are employed (11).

Figure 15 shows two first-order all-pass circuits based on operational amplifiers (op-amps) (12, 13, also see ***Active filters***). The transfer functions are given by $T_a = (Z_2 - kR_1)/(Z_2 + R_1)$ and $T_b = (-kZ_1 + R_2)/(Z_1 + R_2)$. Thus, if Z_2 in Fig. 15(a) or if Z_1 in Fig. 15(b) are selected to be the impedances of capacitors and $k = 1$, then first-order all-pass circuits are realized. The circuit in Fig. 15(a) can be used

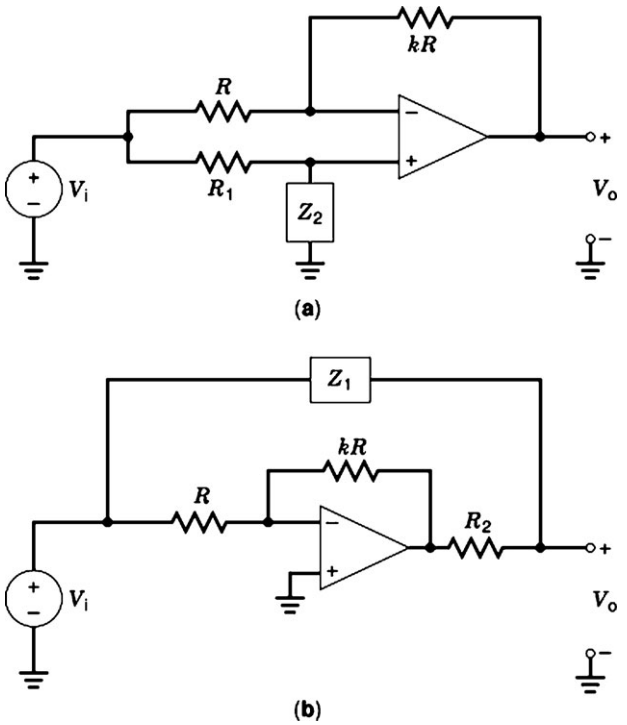

Figure 15. Single op-amp active realizations of first-order all-pass filters. (a) First-order all-pass circuit with gain factor equal to +1. (b) First-order circuit with gain factor equal to −1.

to realize the all-pass circuits used in Figs. 10 and 12. Both circuits in Fig. 15 can be modified to realize second-order inductorless all-pass transfer functions, but the poles and zeros are confined to the real axis. Resistor R_1 in Fig. 15(a) and resistor R_2 in Fig. 15(b) are replaced by RC impedances Z_1 and Z_2, respectively. The circuit in Fig. 15(a) is clearly related to the all-pass circuit shown in Fig. 13. An op-amp has been employed so that the input and output voltages have a common point of reference.

The realization of inductorless second-order all-pass circuits with complex poles can be achieved with the circuits shown in Fig. 16. These circuits are minimal in the number of capacitors required. If the op-amps are ideal in the sense of having infinite gain-bandwidth product, then both circuits have the same transfer function, namely,

$$\frac{V_0}{V_i} = a\left[\frac{s^2 + s\left(\frac{1}{C_1R_2} + \frac{1}{C_2R_2} + \frac{a-1}{aC_2R_1}\right) + \frac{1}{C_1C_2R_1R_2}}{s^2 + s\left(\frac{1}{C_1R_2} + \frac{1}{C_2R_2}\right) + \frac{1}{C_1C_2R_1R_2}}\right] \tag{42}$$

where

$$a = \frac{R_B}{R_A + R_B} < 1 \tag{43}$$

In order to obtain an all-pass transfer function, we must impose the requirement

$$\frac{R_A}{R_B} = 2\frac{R_1}{R_2}\left(1 + \frac{C_2}{C_1}\right) \tag{44}$$

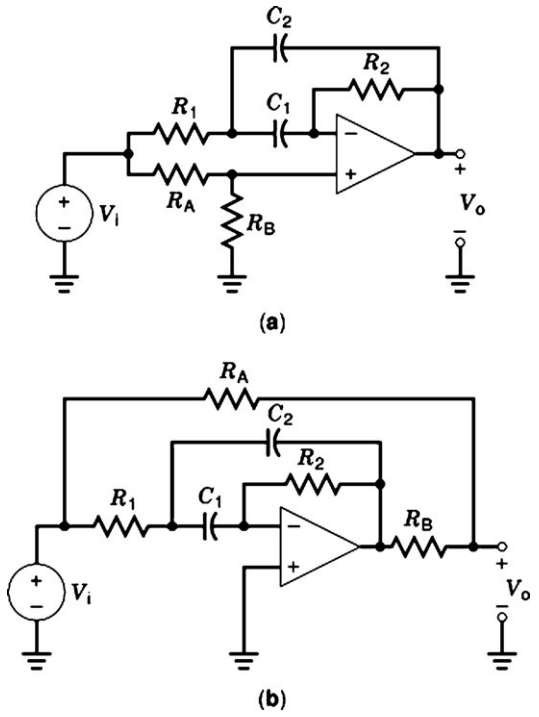

Figure 16. Op-amp circuits for the realization of inductorless second-order all-pass filters with complex poles. (a) Circuit useful in low Q applications in which a light load must be driven. (b) Circuit employed in higher Q applications, but it requires a buffer if a load must be driven.

If Eq. (44) is satisfied, then Eq. (42) becomes

$$\frac{V_0}{V_i} = a\left[\frac{s^2 - s\dfrac{\omega_0}{Q} + \omega_0^2}{s^2 + s\dfrac{\omega_0}{Q} + \omega_0^2}\right] \tag{45}$$

where

$$\omega_0^2 = \frac{1}{C_1C_2R_1R_2}, \quad \frac{1}{Q} = \sqrt{\frac{R_1}{R_2}}\left(\sqrt{\frac{C_1}{C_2}} + \sqrt{\frac{C_2}{C_1}}\right) \tag{46}$$

Although both circuits have the same transfer function when the op-amp is ideal, there are differences in the circuits. The circuit in Fig. 16(a) can drive light loads without an output buffer (14), whereas the circuit in Fig. 16(b) requires a buffer for such loads (15). However, it can be shown that when the finite op-amp gain-bandwidth product is taken into account, the circuit in Fig. 16(b) is better suited for the realization of all-pass transfer functions with poles having a Q greater than about five. Since the Qs required for phase equalization of low-pass filters are usually quite low, the circuit in Fig. 16(a) is a good choice for that application.

If the requirement for a minimum number of capacitors is relaxed, then many inductorless active circuits are available that can realize second-order all-pass transfer functions with complex poles. The interested reader is invited to consult Ref. 16. In fact, if a second-order bandpass circuit is available which has a negative gain factor, then

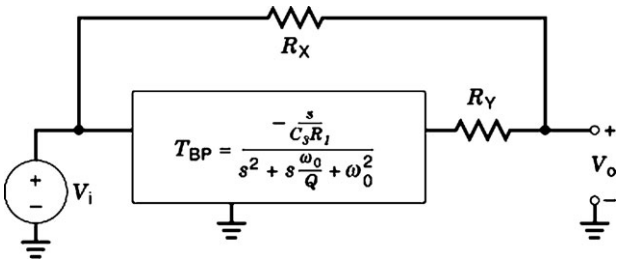

Figure 17. Second-order all-pass circuit realization based on a bandpass filter circuit with negative gain factor.

a second-order all-pass can be realized by summing the output of the bandpass filter with the input signal. Figure 17 shows an all-pass realization using this scheme that is based on the bandpass filter described earlier in this article. The transfer function is

$$\frac{V_0}{V_i} = \frac{R_Y}{R_X + R_Y}\left[\frac{s^2 + s\left(\dfrac{\omega_0}{Q} - \dfrac{1}{C_3R_1}\dfrac{R_X}{R_Y}\right) + \omega_0^2}{s^2 + s\dfrac{\omega_0}{Q} + \omega_0^2}\right] \tag{47}$$

where ω_0 and Q are given in Eq. (37). To obtain an all-pass filter, R_X and R_Y must satisfy

$$\frac{R_Y}{R_X} = \frac{C_1}{2C_3} \tag{48}$$

It is seen that this same scheme is employed in the all-pass filter circuit depicted in Fig. 16(b). If a second-order band-pass filter is available that has a positive gain factor, then a second-order all-pass filter can be obtained by "interchanging input and ground" (17).

Operational transconductance amplifiers (*OTA*s) can also be used to obtain active circuit realizations of voltage-mode all-pass filters. These active devices are approximations to differential-input voltage-controlled current sources (18, 19) and ideally have infinite input and output impedances. Figure 18 shows circuit configurations for a first-order and a second-order all-pass filter. If the OTAs are ideal, the transfer function for the first-order filter is

$$\frac{V_2}{V_i} = \frac{sC - g_{m1}}{sC + g_{m2}} \tag{49}$$

where g_{m1} and g_{m2} are the transconductances of OTA1 and OTA2, respectively. The transconductance is controlled by a control current that is applied to a terminal (not shown) of the OTA. Ideally, the transconductance is constant for a constant control current. If the control currents for the OTAs in Fig. 18(a) are adjusted so that $g_{m1} = g_{m2}$, then a first-order all-pass filter is obtained. The transfer function for the circuit shown in Fig. 18(b) is

$$\frac{V_0}{V_i} = \frac{s^2C_1C_2g_{m4} + s(C_2g_{m1}g_{m3} - C_1g_{m2}g_{m4}) + g_{m1}g_{m2}g_{m4}}{s^2C_1C_2g_{m5} + sC_2g_{m1}g_{m3} + g_{m1}g_{m2}g_{m4}} \tag{50}$$

To obtain a second-order all-pass circuit, the transconductances in Fig. 18(b) must satisfy

$$C_1g_{m2}g_{m4} = 2C_2g_{m1}g_{m3} \tag{51}$$

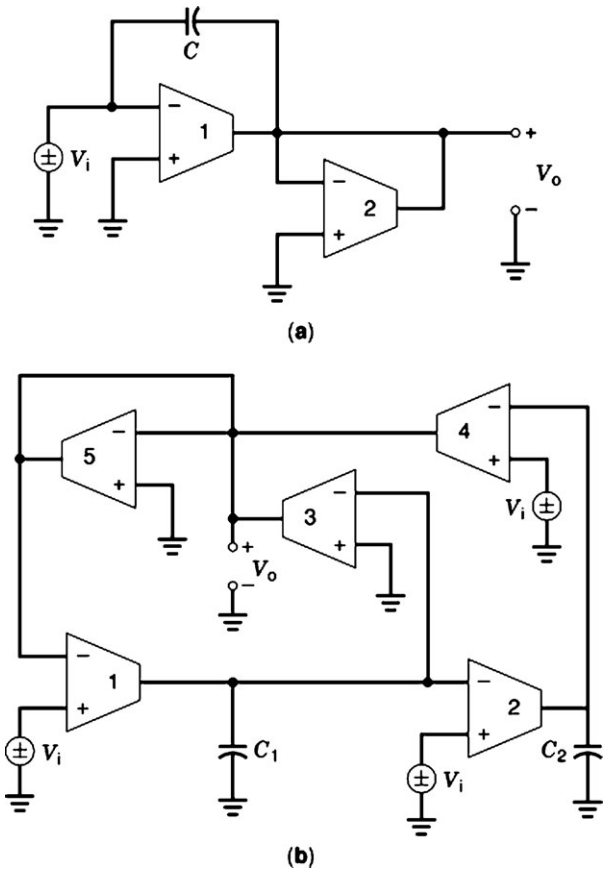

Figure 18. Operational transconductance amplifier (*OTA*) all-pass filter realizations. (a) First-order all-pass circuit. (b) Second-order all-pass circuit.

and $g_{m4} = g_{m5}$. For realizing integrated circuit versions of filters (see ***Analog processing circuits***), OTAs are particularly suited, because they are relatively simple in structure, and they can operate at higher frequencies than, say, voltage-mode op-amps. However, OTAs depart from ideal in many aspects, of which the chief aspects are finite input and output impedances, a frequency-dependent transconductance, and a limited range of input signal that is allowed for linear operation. The input and output impedances also are dependent on the control current (18, 19). The nonideal characteristics of OTAs must be taken into account in the design of most circuits if accurate results are to be obtained.

Voltage-mode all-pass filters can also be constructed using current-feedback op-amps (*CFOA*s). Soliman (20) provides several useful realizations.

Current-mode Realizations

All-pass filters in which the input and output variables of interest are currents are called current-mode circuits. If, in addition, the variables of interest throughout the circuit are currents, then the current is a fully current-mode circuit. Active, fully current-mode circuits are of interest because they offer a larger bandwidth if properly designed than do active voltage-mode circuits (21). Passive current-mode all-pass filters are easily obtained from passive voltage-mode filters because the networks are reciprocal. Thus, if the output port of the voltage-mode circuit is excited by a current source and if the input port of the voltage-mode circuit is shorted with the output current flowing through this short, then the current transfer function of the resulting circuit is the same as the voltage-mode transfer function of the original circuit. However, the input and output currents do not have a common ground. Active current-mode all-pass filters with a common ground can be obtained from voltage-mode filters that incorporate a voltage amplifier by using the adjoint network concept (22). For example, the application of the adjoint network concept to the first-order voltage-mode all-pass circuit in Figure 15(b) results in the fully current-mode all-pass circuit shown in Fig. 19(a). This first-order all-pass filter employs a second-generation, positive current conveyor (CCII+) as the active device (see ***Current conveyors***). The transfer function of the circuit is

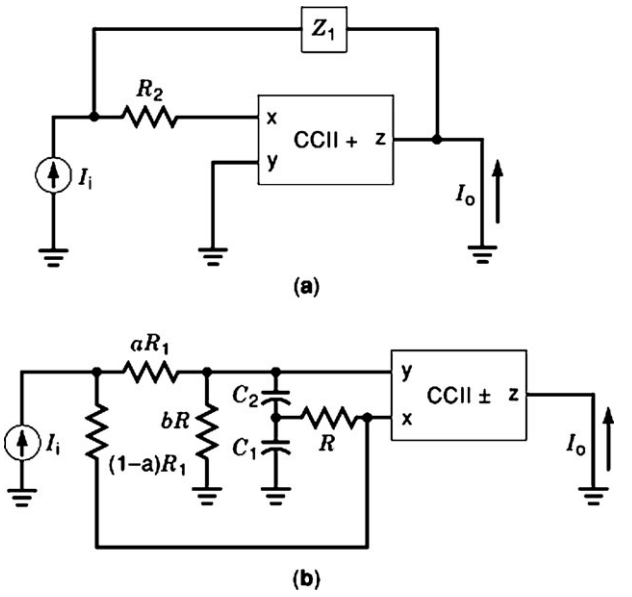

Figure 19. Current-mode all-pass circuits. (a) First-order. (b) Second-order.

$$\frac{I_0}{I_i} = \frac{Z_1 - R_2}{Z_1 + R_2} \tag{52}$$

If Z_1 is chosen as $(1/(sC)$, then a first-order current-mode all-pass filter is obtained. Although the all-pass filter in Fig. 19(a) uses the minimum number of passive elements, the capacitor is not counted as a grounded capacitor (a capacitor in which one lead of the capacitor has its own connection to ground), because it is connected to ground only through the output lead. If this circuit is cascaded with another circuit, the output lead may be connected to a virtual ground, and in this case, the capacitor would not be a physically grounded one. Other first-order all-pass realizations that incorporate one (grounded) capacitor and use one CCII have been given (23), although they employ four resistors. These realizations are easily cascaded.

A second-order all-pass filter that uses only one CCII is shown in Fig. 19(b). This circuit can realize complex poles

and uses the minimum number of capacitors (23). Note that no feedback elements are connected to the output terminal z of the current conveyor, and so this all-pass realization can be easily cascaded to achieve higher order realizations. Either a positive or a negative current conveyor can be employed. The transfer function of the circuit is given by

$$\frac{I_0}{I_i} = \pm a \left[\frac{s^2 + s\dfrac{(C_2 - kC_1)}{bC_1C_2R} + \dfrac{1}{bC_1C_2R^2}}{s^2 + s\dfrac{C_1 + C_2}{bC_1C_2R} + \dfrac{1}{bC_1C_2R^2}} \right] \tag{53}$$

where a and b are identified in Fig. 19(b) and k is

$$k = \frac{b}{a}(1 - a) - 1$$

The plus sign is chosen if a CCII+ is used, and the minus sign is chosen if a CCII− is utilized.

To realize an all-pass transfer function, the elements must also satisfy

$$\frac{C_2}{C_1} = \frac{b}{2a} - \left(1 + \frac{b}{2}\right) = \frac{k - 1}{2}$$

Minimum passive sensitivities are obtained with $C_1 = C_2$, but the spread of element values can be reduced for larger Qs by choosing C_2 larger than C_1.

CCIIs are simpler to construct than first-generation current conveyors (CCIs), and so are much more widely used. However, a second-order all-pass filter with complex poles can be realized using a single CCI (24). This circuit uses the minimum number of capacitors, and both capacitors are grounded.

MINIMUM PHASE AND ALL-PASS FILTERS

We say that a real, rational, stable transfer function in s is a minimum phase transfer function if all its zeros are confined to the closed LHP. No zeros are allowed in the RHP. On the other hand, a nonminimum phase transfer is one that has one or more zeros in the RHP. An all-pass transfer function is nonminimum phase. Figure 20 depicts pole-zero diagrams for minimum phase [Figs. 20(a) and (c)] and nonminimum phase [Figs. 20(b) and (d)] transfer functions. To convert the diagram in Fig. 20(a) to a diagram corresponding to a nonminimum phase transfer function with the same magnitude characteristic, we reflect the zeros in Fig. 20(a) through the origin. Thus, $z_3 = -z_1$ and $z_4 = -z_2$ in Fig. 20(b). The corresponding transfer functions have the same magnitude characteristics because the lengths of the vectors from the zeros z_1 and z_2 to an arbitrary point P on the $j\omega$ axis in Fig. 20(a) are the same as the lengths of the vectors from the zeros z_3 and z_4 to P in Fig. 20(b). However, considering the order of the transfer functions (third order) and that both have the same magnitude characteristic, there is more phase lag associated with the pole-zero diagram in Fig. 20(b) than with Fig. 20(a).

In Figs. 20(c) and 20(d), a pair of complex poles, labeled p_1 and p_2, has been reflected into the RHP as zeros labeled z_1 and z_2, where $z_1 = -p_1$ and $z_2 = -p_2$. The phase characteristics of the corresponding transfer functions are the same, but the magnitude characteristics differ. Still, the second-order transfer function corresponding to Fig. 20(d) is a nonminimum phase one. Note that it has the same phase as the fourth-order transfer function corresponding to Fig. 20(c).

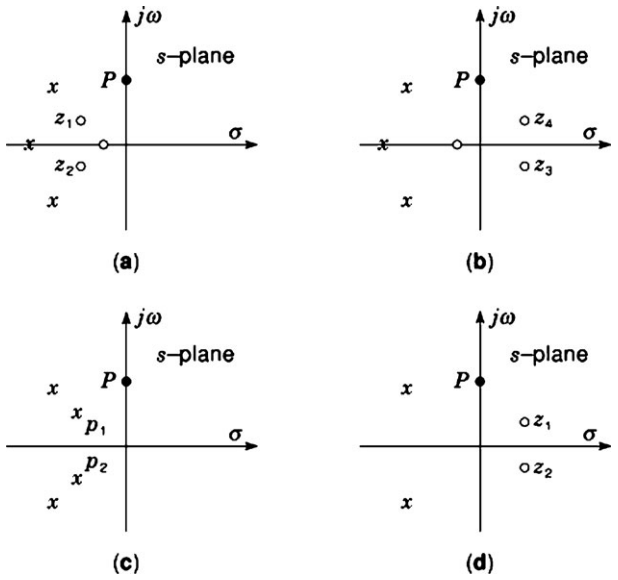

Figure 20. Transfer function pole-zero plots. (a) and (c) Plots for minimum phase transfer functions. (b) and (d) Plots for nonminimum phase transfer functions. The transfer functions corresponding to the plots in (a) and (b) have the same magnitude characteristics but differ in phase characteristics. The transfer functions corresponding to the plots in (c) and (d) have the same phase characteristics but differ in magnitude characteristics.

A nonminimum phase transfer function can be expressed as the product of a minimum phase transfer function and an all-pass transfer function. For example, suppose we have the transfer function

$$T(s) = \frac{(s-1)[(s-3)^2 + 1]}{[(s+1)^2 + 1][(s+2)^2 + 1]}$$

By multiplying $T(s)$ by

$$\frac{(s+1)[(s+3)^2 + 1]}{(s+1)[(s+3)^2 + 1]} = 1$$

and regrouping the factors, we obtain

$$\begin{aligned} T(s) &= \frac{(s+1)[(s+3)^2 + 1]}{[(s+1)^2 + 1][(s+2)^2 + 1]} \cdot \frac{(s-1)[(s-3)^2 + 1]}{(s+1)[(s+3)^2 + 1]} \\ &= T_{MP}T_{AP} \end{aligned}$$

where $T_{MP}(s)$ is a minimum phase transfer function and $T_{AP}(s)$ denotes an all-pass transfer function.

For sinusoidal steady state analysis applications, a minimum phase transfer function $T(s)$ can be expressed in the form

$$T(j\omega) = e^{[-\alpha(\omega) - j\theta(\omega)]} \tag{54}$$

where $\alpha(\omega)$ is the attenuation function in nepers and $\theta(\omega)$ is the negative of the phase function in radians. These two functions are not independent but are related by the

Hilbert transforms given by

$$\alpha(\omega) = \alpha(\infty) + \alpha(0) - \frac{\omega^2}{\pi}\int_{-\infty}^{\infty} \frac{\theta(\Omega)}{\Omega(\Omega^2 - \omega^2)}\, d\Omega \tag{55a}$$

$$\theta(\omega) = \frac{\omega}{\pi}\int_{-\infty}^{\infty} \frac{\alpha(\Omega)}{\Omega^2 - \omega^2}\, d\Omega \tag{55b}$$

where Ω is a dummy variable and $\alpha(0)$ is the value of the attenuation function at zero frequency (25). Equations 55a and 55b show that if $\alpha(\omega)$ is specified for all ω, then $\theta(\omega)$ is also specified over all ω for a minimum phase transfer function. Thus, $\alpha(\omega)$ and $\theta(\omega)$ cannot be specified independently. Even if $\alpha(\omega)$ is specified over only part of the $j\omega$ axis and $\theta(\omega)$ is specified over the remaining parts, then $T(j\omega)$ is determined over the whole axis.

However, attenuation and phase are independent of each other in the case of nonminimum phase transfer functions. This is the reason that nonminimum phase transfer functions usually are used to meet simultaneous attenuation and phase specifications (26). Nevertheless, all-pole low-pass minimum phase transfer functions can serve as useful prototypes for all-pass filters (27). An all-pole filter has a transfer function given by

$$T(s) = \frac{H}{q(s)} = \frac{H}{m(s) + n(s)} \tag{56}$$

where we take the gain factor H to be positive for convenience, and $m(s)$ and $n(s)$ are the even and odd parts of the denominator polynomial $q(s)$, respectively. The phase of this low-pass filter is given by

$$\theta(\omega) = -\tan^{-1}\left[\frac{n(j\omega)/j}{m(j\omega)}\right] \tag{57}$$

An all-pass transfer function constructed from this low-pass transfer function has the form

$$T_{AP}(s) = \frac{m(s) - n(s)}{m(s) + n(s)} \tag{58}$$

and has a phase characteristic that can be expressed as

$$\theta_{AP}(\omega) = -2\tan^{-1}\left[\frac{n(j\omega)/j}{m(j\omega)}\right] \tag{59}$$

Thus, the phase and delay characteristics are the same as for the low-pass prototype transfer function except for the factor of two. Suppose that the low-pass prototype is a Bessel filter transfer function. Then an all-pass transfer function can be devised that also has maximally flat delay at $\omega = 0$ and which has, ideally, a lossless magnitude characteristic. For example, the third-order Bessel filter transfer function is

$$T(s) = \frac{15}{s^3 + 6s^2 + 15s + 15}$$

Thus, the corresponding all-pass transfer function is

$$T_{AP}(s) = \frac{-s^3 + 6s^2 - 15s + 15}{s^3 + 6s^2 + 15s + 15}$$

The Bessel filter produces a 1-s delay, and the all-pass filter generates a 2-s delay, but the delay in both cases is maximally flat at $\omega = 0$.

DIGITAL ALL-PASS FILTERS

Digital filters can be classed into two categories: finite impulse response (*FIR*) filters and infinite impulse response (*IIR*) filters (see ***Digital filters***). The FIR filters can be designed with perfectly linear phase. However, in general, stable, realizable IIR filters cannot achieve perfectly linear phase. Although IIR filters can be designed to approximate given magnitude and phase requirements, a popular approach to digital filter design is to base a design on continuous time filter approximations and transform the result to digital filter form. Then the phase is linearized (equalized) using cascaded digital all-pass filters. This approach is a practical one (among several practical approaches) if the order of the all-pass filter required is reasonable (28).

To devise a first-order, real, stable, all-pass transfer function, we place a zero outside the unit circle in the z plane on the real axis at $z = (1/r_1)$ corresponding to a pole at $z = r_1$, $|r_1| < 1$. The resulting transfer function is given by

$$H(z) = \frac{z - \dfrac{1}{r_1}}{z - r_1} = \frac{1}{r_1}\left(\frac{zr_1 - 1}{z - r_1}\right) \tag{60}$$

or

$$H(z) = \frac{-z}{r_1}\left(\frac{1 - \dfrac{z^{-1}}{r_1}}{1 - \dfrac{z}{r_1}}\right) \tag{61}$$

Evaluating $H(z)$ in Eq. (68) for $z = e^{j\omega T}$, where T is the sampling interval, we obtain

$$H(e^{j\omega T}) = \frac{-e^{j\omega T}}{r_1}\left(\frac{r_1 - e^{-j\omega T}}{r_1 - e^{j\omega T}}\right) \tag{62}$$

The numerator of the term in parentheses in Eq. (69) is the conjugate of the term in the denominator. Thus, the magnitude of the term in parentheses is one. Also, the magnitude of $-e^{j\omega T}$ is one. As a result, we have $|H(e^{j\omega T})| = 1/|r_1|$. The phase, denoted as $\beta(\omega)$, for r_1 assumed to be positive is obtained from Eq. (69) as

$$\beta(\omega) = \pi + \omega T + 2\tan^{-1}\left[\frac{\sin\omega T}{r_1 - \cos\omega T}\right] \tag{63}$$

Since the magnitude characteristic is a constant over frequency and yet the phase characteristic changes as a function of frequency as can be seen from Eq. (70), the transfer function in Eq. (67) is an all-pass one.

A second-order, real, stable all-pass transfer function with complex poles can be devised in a manner similar to that used for the first-order transfer function. For a complex pole at $z = re^{j\theta}$, $0 < \theta < \pi$, we must have another pole at $z = re^{-j\theta}$ if the transfer function is to be real. We take r positive for convenience and $r < 1$ for stability. Thus, for each pair of complex poles given by $z = re^{\pm j\theta}$, we place a pair

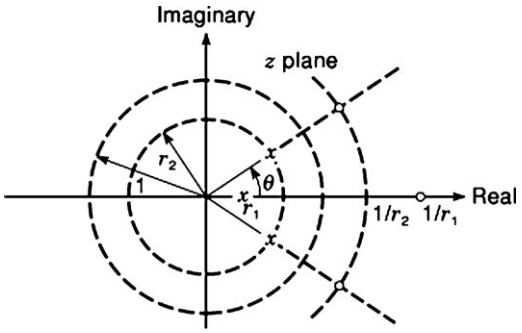

Figure 21. Poles and zeros of a digital third-order all-pass filter transfer function.

of complex zeros outside the unit circle at $z = (1/r)e^{\pm j\theta}$. The resulting transfer function is given by

$$H(z) = \frac{\left(z - \frac{1}{r}e^{j\theta}\right)\left(z - \frac{1}{r}e^{-j\theta}\right)}{(z - re^{j\theta})(z - re^{-j\theta})} \tag{64}$$

which can be rearranged into

$$H(z) = \frac{z^2}{r^2}\left(\frac{1 - \frac{2\cos\theta}{r}z^{-1} + \frac{z^{-2}}{r^2}}{1 - \frac{2\cos\theta}{r}z + \frac{z^2}{r^2}}\right) \tag{65}$$

The magnitude characteristic is easily obtained by evaluating $H(z)$ in Eq. (72) for $z = e^{j\omega T}$. The result is $|H(e^{j\omega T})| = 1/r^2$, and the phase is given by

$$\begin{aligned}\beta(\omega) = {} & 2\omega T + 2\tan^{-1}\left[\frac{\sin(\omega T + \theta)}{r - \cos(\omega T + \theta)}\right] \\ & + 2\tan^{-1}\left[\frac{\sin(\omega T + \theta)}{r - \cos(\omega T + \theta)}\right]\end{aligned} \tag{66}$$

A pattern is indicated by Eqs. 68 and 72 for higher order, real, stable all-pass transfer functions. Let N be the order of the all-pass transfer function, and let the poles be inside the unit circle and occur in conjugate pairs if complex. That is, each complex pole pair is described by

$$z = r_i e^{\pm j\theta_i}, \quad i = 1, 2, \ldots, m \tag{67}$$

where $0 \le m \le N/2$ and $0 < r_i < 1$. Then the transfer function is given by

$$H(z) = \frac{z^N}{k}\left(\frac{1 + \sum_{i=1}^{N} a_i z^{-i}}{1 + \sum_{i=1}^{N} a_i z^{i}}\right) \tag{68}$$

where k is given by

$$k = (-1)^N \prod_{i=1}^{N} r_i \tag{69}$$

and all the coefficients a_i in Eq. (75) are real. The magnitude characteristic of the transfer function in Eq. (75) evaluated for $z = e^{j\omega T}$ is $1/|k|$. Figure 21 shows a pole-zero plot on the z plane for an all-pass transfer function with a real pole at $z = r_1$ and two conjugate complex poles at $z = r_2 e^{\pm j\theta}$. The transfer function is real and stable.

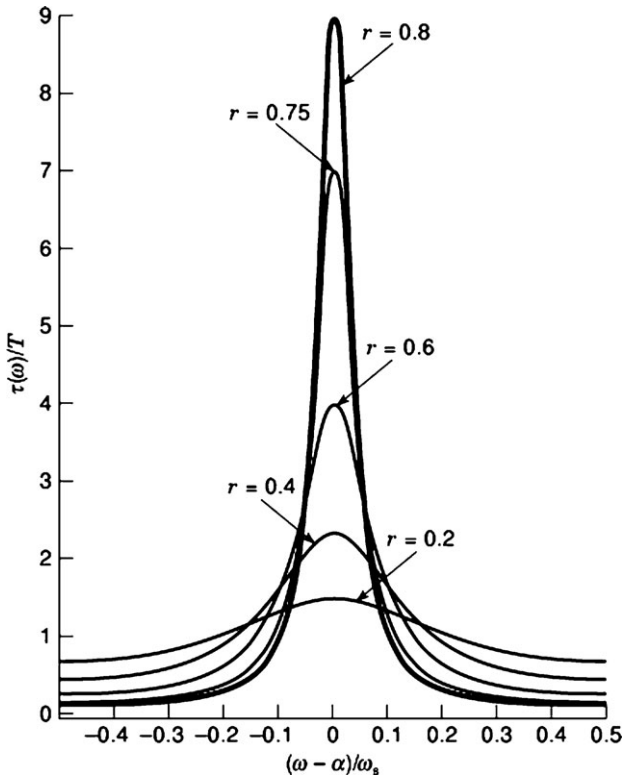

Figure 22. Plots of the first function to the right of the equal sign in Eq. (70) for values of r = 0.2, 0.4, 0.6, 0.75, and 0.8.

The delay of an IIR digital filter can be made more flat by connecting all-pass filters in cascade. The coefficients required for the all-pass filters as well as the number of all-pass filters needed are best determined by a cut-and-try process using a computer program that plots delay characteristics interactively and quickly. However, an aid for delay equalization can be established. For this purpose, let θ in the transfer function for a second-order all-pass transfer function in Eq. (71) be expressed in terms of the sampling interval T as $\theta = \alpha T$. Then the normalized time delay characteristic can be obtained from $-d\beta/d\omega$ applied to Eq. (73). Thus, we have

$$\frac{\tau(\omega)}{T} = \frac{1 - r^2}{1 + r^2 - 2r\cos T(\omega - \alpha)} + \frac{1 - r^2}{1 + r^2 - 2r\cos T(\omega + \alpha)} \tag{70}$$

Equation (77) expresses the normalized delay as the sum of two functions. Let us examine the first function to the right of the equal sign. Its maximum value is $(1 + r)/(1 - r)$, which occurs at $\omega = \alpha$ in $-\pi \le \omega T \le \pi$. Since the delay characteristics obtained from cascaded all-pass filters are described by a sum of functions of this type, a convenient design aid (29) is obtained by plotting this function for several values of r. These plots are shown in Fig. 22. The frequency axis has been normalized to $(\omega - \alpha)/\omega_s$, where ω_s is the sampling frequency given by $\omega_s = 2\pi/T$.

As an illustration of the concept, we apply delay equalization to a bandpass filter transfer function (8) given by

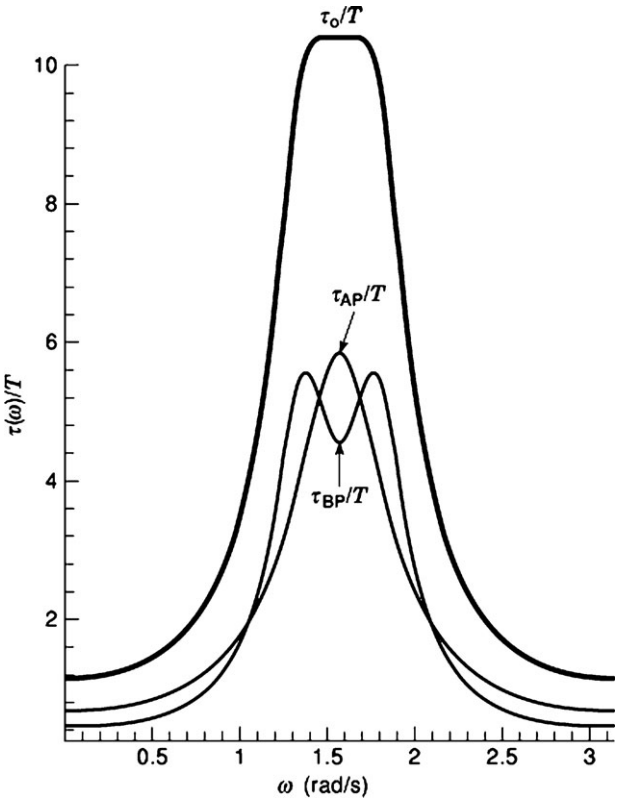

Figure 23. Equalizing the delay characteristic of a bandpass filter in the neighborhood of its center frequency with a second-order all-pass filter.

$$H(z) = \frac{0.021z^{-4} - 0.178z^{-2} + 0.021}{0.349z^{-4} - 0.979z^{-2} + 0.849}$$

This filter has its center frequency at $\omega = \omega_s/4$ and has a bandwidth described by $0.2\omega_s \leq \omega \leq 0.3\omega_s$. The normalized delay characteristic of the bandpass filter is denoted by τ_{BP}/T and is shown in Fig. 23. It is clear that this characteristic would benefit by the addition of a delay lump from a second-order all-pass filter located at $\omega = \omega_s/4$ with $r = 0.7$. That is, a second-order all-pass filter is utilized with normalized delay characteristic given by Eq. (77) with $\alpha = \omega_s/4$ and $r = 0.7$. The normalized delay characteristic of the all-pass filter is labeled τ_{AP}/T in Fig. 23. The resulting overall normalized delay characteristic, denoted by τ_o/T, is also shown, and it is seen that the result is flatter in the neighborhood of the center frequency at the expense of the characteristic at the edges of the bandpass filter passband. Additional all-pass delay lumps can be employed to correct the delay at the band edges.

First- and second-order digital all-pass filters can be realized using the structures shown in Fig. 24. Figure 24(a) shows a realization for a first-order filter that employs only one delay (30). Its transfer function is

$$\frac{Y}{X} = H(z) = z\left(\frac{a_1 - z^{-1}}{a_1 - z}\right) \tag{71}$$

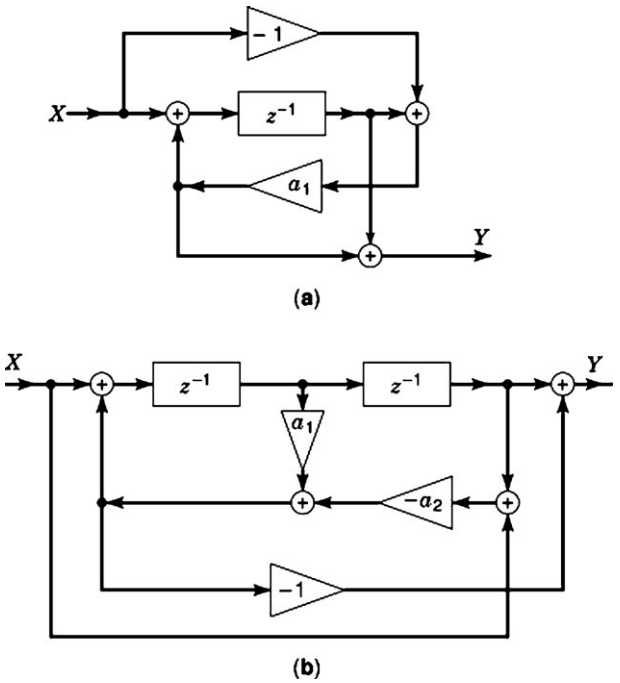

Figure 24. Digital all-pass filter realizations. (a) First-order realization. (b) Second-order realization.

where X and Y are the input and output variables, respectively, and a_1 is the coefficient of a multiplier. The structure in Fig. 24(b) can be used to realize second-order all-pass transfer functions. Its transfer function is given by

$$\frac{Y}{X} = H(z) = z^2\left(\frac{a_2 - a_1z^{-1} + z^{-2}}{a_2 - a_1z + z^2}\right) \tag{72}$$

Both structures in Fig. 24 are minimal in the number of delays required. Higher order all-pass filters can be constructed by cascading first- and second-order realizations. There are many other structures that can be used to realize first- and second-order all-pass filters; an extensive catalog of such structures is given in Ref. 30, and a discussion of the effects of multiplication roundoff and hardware requirements is provided.

BIBLIOGRAPHY

1. A. Budak *Active and Passive Network Analysis and Synthesis*, Boston: Houghton Mifflin, 1974; reprinted Prospect Heights, IL: Waveland Press, 1991.
2. H. J. Blinchikoff A. I. Zverev *Filtering in the Time and Frequency Domains*, New York: Wiley, 1976; reprinted Malabar, FL: Robert E. Krieger, 1987.
3. M. S. Ghausi K. R. Laker *Modern Filter Design*, Englewood Cliffs, NJ: Prentice-Hall, 1981.
4. P. Klemp Phase shifter yields slope-polarity detection, *EDN*, **41** (6): 92, 94, 96, 1996.
5. D. J. Comer J. E. McDermid Inductorless bandpass characteristics using all-pass networks, *IEEE Trans. Circuit Theory*, **CT-15** (4), 501–503, 1968.
6. D. T. Comer D. J. Comer J. R. Gonzalez A high-frequency integrable bandpass filter configuration, *IEEE Trans. Circuits Syst. II, Analog Digit. Signal Process.*, **44** (10): 856–860, 1997.
7. A. Budak *Circuit Theory Fundamentals and Applications*, 2nd ed, Englewood Cliffs, NJ: Prentice-Hall, 1987.
8. H. Lam *Analog and Digital Filters*, Englewood Cliffs, NJ: Prentice-Hall, 1979.
9. P. Aronhime A one-transistor all-pass network, *Proc. IEEE*, **55**: 445–446, 1967.
10. H. J. Orchard Active all-pass networks with constant resistance, *IEEE Trans. Circuit Theory*, **CT-20**: 177–179, 1973.
11. H. Rubin R. K. Even Single-transistor all-pass networks, *IEEE Trans. Circuit Theory*, **CT-20**: 24–30, 1973.
12. R. Genin Realization of an all-pass transfer function using operational amplifiers, *Proc. IEEE*, **56**: 1746–1747, 1968.
13. P. Aronhime A. Budak An operational amplifier all-pass network, *Proc. IEEE*, **57**: 1677–1678, 1969.
14. T. Deliyannis RC active allpass sections, *Electron. Lett.*, **5** (3): 59–60, 1969.
15. A. Budak P. Aronhime Frequency limitations on an operational amplifier realization of all-pass transfer functions with complex poles, *Proc. IEEE*, **58**: 1137–1138, 1970.
16. G. S. Moschytz A general all-pass network based on Sallen-Key circuit, *IEEE Trans. Circuit Theory*, **CT-19**: 392–394, 1972.
17. D. Hilberman Input and ground as complements in active filters, *IEEE Trans. Circuit Theory*, **CT-20**: 540–547, 1973.
18. R. Schauman M. S. Ghausi K. R. Laker *Design of Analog Filters*, Englewood Cliffs, NJ: Prentice-Hall, 1990.
19. P. Aronhime Applications of operational amplifiers. InJ. C. Whitaker (ed.), *The Electronics Handbook*, 2nd Ed. Boca Raton, FL: CRC Press, 2005.
20. A. M. Soliman Applications of the current feedback operational amplifiers, *Analog Integr. Circuits Signal Process.*, **11**: 265–302, 1996.
21. C. ToumazouF. J. LidgeyD. G. Haigh eds.,*Analogue IC Design: The Current-Mode Approach*, London: Peter Peregrinus, 1990.
22. G. W. Roberts A. S. Sedra All current-mode frequency selective circuits, *Electron. Lett.*, **25** (12): 759–761, 1989.
23. A. M. Soliman Generation of current conveyor-based all-pass filters from op amp-based circuits, *IEEE Trans. Circuits Syst. II, Analog Digit. Signal Process.*, **44**: 324–330, 1997.
24. P. Aronhime D. Nelson J. Zurada C. Adams Realization of current-mode complex pole all-pass networks using a single current conveyor. In *Proceedings of the International Symposium on Circuits and Systems*, vol.**4**, 1990, pp. 3193–3196.
25. C. S. Lindquist *Active Network Design*, Long Beach, CA: Steward & Sons, 1977.
26. A. S. Sedra P. O. Brackett *Filter Theory and Design: Active and Passive*, Portland: Matrix Publishers, 1978.
27. L. P. Huelsman *Active and Passive Analog Filter Design*, New York: McGraw-Hill, 1993.
28. L. R. Rabiner B. Gold *Theory and Application of Digital Signal Processing*, Englewood Cliffs, NJ: Prentice-Hall, 1975.
29. S. A. Tretter *Introduction to Discrete-Time Signal Processing*, New York: Wiley, 1976.
30. S. K. Mitra K. Hirano Digital all-pass networks, *IEEE Trans. Circuits Syst.* **CAS-21**: 688–700, 1974.

Reading List

W.-K. Chen ed., *The Circuits and Filters Handbook*, Boca Raton, FL: CRC Press, 1995.

A. B. Williams F. J. Taylor *Electronic Filter Design Handbook*, New York: McGraw-Hill, 1995.

PETER ARONHIME
University of Louisville, 10 Eastern Parkway, Louisville, KY, 40292